HGT

Safety of Direct Intraparenchymal AAVrh.10-Mediated Central Nervous System Gene Therapy for Metachromatic Leukodystrophy

Jonathan B. Rosenberg,[1] Alvin Chen,[1] Bishnu P. De,[1] Jonathan P. Dyke,[2] Douglas J. Ballon,[2] Sebastien Monette,[3] Rodolfo J. Ricart Arbona,[3] Stephen M. Kaminsky,[1] Ronald G. Crystal,[1] and Dolan Sondhi[1,*]

[1]Department of Genetic Medicine, Weill Cornell Medical College, New York, New York, USA; [2]Department of Radiology, Citigroup Biomedical Imaging Center, Weill Cornell Medical College, New York, New York, USA; [3]Center for Comparative Medicine and Pathology, Memorial Sloan Kettering Cancer Center and Weill Cornell Medicine, New York, New York, USA.

Metachromatic leukodystrophy, a fatal pediatric neurodegenerative lysosomal storage disease caused by mutations in the arylsulfatase A (ARSA) gene, is characterized by intracellular accumulation of sulfatides in the lysosomes of cells of the central nervous system (CNS). In previous studies, we have demonstrated efficacy of AAVrh.10hARSA, an adeno-associated virus (AAV) serotype rh.10 vector coding for the human ARSA gene to the CNS of a mouse model of the disease, and that catheter-based intraparenchymal administration of AAVrh.10hARSA to the CNS of nonhuman primates (NHPs) white matter results in widespread expression of ARSA. As a formal dose-escalating safety/toxicology study, we assessed the safety of intraparenchymal delivery of AAVrh.10hARSA vector to 12 sites in the white matter of the CNS of NHPs at 2.85×10^{10} (total low dose, 2.4×10^9 genome copies [gc]/site) and 1.5×10^{12} (total high dose, 1.3×10^{11} gc/site) gc, compared to AAVrh.10Null (1.5×10^{12} gc total, 1.3×10^{11} gc/site) as a vector control, and phosphate buffered saline for a sham surgical control. No significant adverse effects were observed in animals treated with low dose AAVrh.10hARSA. However, animals treated with the high dose AAVrh.10ARSA and the high dose Null vector had highly localized CNS abnormalities on magnetic resonance imaging scans at the sites of catheter infusions, and histopathology demonstrated that these sites were associated with infiltrates of T cells, B cells, microglial cells, and/or macrophages. Although these findings had no clinical consequences, these safety data contribute to understanding the dose limits for CNS white matter direct intraparenchymal administration of AAVrh.10 vectors for treatment of CNS disorders.

Keywords: metachromatic leukodystrophy (MLD), toxicology, adeno-associated virus (AAV), arylsulfatase A (ARSA), central nervous system (CNS), safety study

INTRODUCTION

METACHROMATIC LEUKODYSTROPHY (MLD) IS an autosomal recessive, fatal, pediatric, neurodegenerative lysosomal storage disease caused by the deficiency of the enzyme arylsulfatase A (ARSA).[1–4] Loss of functional ARSA-mediated enzymatic breakdown of sulfatides triggers an intracellular accumulation of toxic sulfatides in the lysosomes of microglia, oligodendrocytes, and Schwann cells, resulting in widespread demyelination in the central nervous system (CNS) and peripheral nervous system (PNS).[5–12]

The focus of this study was to assess in nonhuman primates (NHPs) the safety of therapy for MLD using direct administration to the CNS parenchyma of an AAVrh.10 vector coding for human ARSA (AAVrh.10-hARSA). Prior work in a murine model of MLD demonstrated that direct AAVrh.10hARSA administration to the CNS ameliorated the disease phenotypes,[13] and a study comparing routes of delivery of AAVrh.10hARSA to the CNS of NHPs concluded that AAVrh.10-mediated delivery of ARSA to the cerebral white matter yielded wide distribution of ARSA.[14]

As the next step in translation of AAVrh.10hARSA therapy to humans, we carried out a safety study with CNS administration of AAVrh.10hARSA in NHP, designed with input from the Center for Biologics Evaluation and Research, Food and Drug Administration (Rockville, MD). The data demonstrate no adverse effects at the clinical, imaging, or histologic levels with intraparenchymal administration of a total dose of 2.85×10^{10} genome copies (gc) divided into doses administered bilaterally to 12 sites in the cerebral

*Correspondence: Dr. Dolan Sondhi, Department of Genetic Medicine, Weill Cornell Medical College, 1300 York Avenue, Box 164, New York, NY 10065, USA. E-mail: geneticmedicine@med.cornell.edu

white matter (2.4×10^9 gc/site). However, at a dose of ~ 500-fold higher (1.5×10^{12} gc in 12 divided doses, 1.3×10^{11} gc/site), adverse effects were localized to the site of administration at the catheter tip characterized by pathologic abnormalities (<2.1% of the total brain volume) using T1-weighted magnetic resonance imaging (MRI) of the brain. Histological assessment demonstrated persistent localized inflammatory cell infiltration. Although periodic videotaped assessment of the NHP over time showed no clinical sequela of these abnormalities, this sets an upper limit to the amount of vector that can be safely administered directly through catheters to the CNS white matter and helps inform the design of a clinical trial of CNS administration of AAVrh.10hARSA to treat MLD.

METHODS

Nonhuman primates

Twenty-four adult *Chlorocebus aethiops sabaeus* NHPs (African Green monkeys; 2- to 4-year-old males ($n = 11$) and females ($n = 13$); 2.5 to 5.5 kg weight at time of arrival) were purchased from the Wake Forest University Primate Center (Winston-Salem, NC). All monkeys were healthy and pathogen-free during the 3-month quarantine period. No animal had been previously used for experimental studies. NHPs were maintained in paired-housed cages, except following surgery when they were individually housed to prevent injuries, fed twice daily with monkey chow (Monkey Diet Jumbo; PMI Nutrition International, Brentwood, MO), supplemented with fruit or vegetables daily, with access to water *ad libitum*, and observed daily by the research specialists for general appearance, signs of toxicity, distress, and changes in behavior. All experiments were approved by Institutional Animal Care and Use Committee of the Weill Cornell Medical College (New York, NY). We used African Green monkeys due to the extensive behavioral and blood parameter datasets from our prior NHP adeno-associated virus (AAV) safety/toxicology studies.[14–18]

Study design

The design of this safety study incorporated FDA guidance provided at a preinvestigational new drug application meeting. AAVrh.10hARSA was administered at two doses into CNS of NHPs through the white matter intraparenchymal route of delivery, with a total dose of 2.85×10^{10} or 1.5×10^{12} gc per NHP, irrespective of weight or gender (the average NHP was ~ 6 kg/males and 4 kg/females at administration). Controls included AAVrh.10-Null (this vector serves as a vector control and is identical to the experimental vector with the exception that the expression cassette is a nontranslatable VEGF intron 5 sequence of vascular endothelial growth factor) and a phosphate buffered saline (PBS) sham surgical control.

Each dose cohort included $n = 8$ NHP (4 males/4 females), except for the control groups (AAVrh.10Null and sham controls) which had an $n = 4$ (1–2 males/2–3 females; Table 1). To maintain a treatment blind for this study, NHPs were randomly assigned into the four cohorts,

Table 1. *Dose, time of assessment, and time of sacrifice of nonhuman primates*

Group	Vector	Total Dose (gc)	n	Time of Assessments (week)[a,b]	Time of Sacrifice (week)[c]
A	AAVrh.10hARSA	2.85×10^{10}	2	Pre, 0, 1	1
			2	Pre, 0, 1, 2, 4, 8, ⑬	13
			2	Pre, 0, 1, 2, 4, 8, 13, ㉖	26
			2	Pre, ⓪ 1, 2, 4, 8, ⑬, ㉖, ㊽	52
B	AAVrh.10hARSA	1.5×10^{12}	2	Pre, 0, 1	1
			2	Pre, 0, 1, 2, 4, 8, ⑬	13
			2	Pre, 0, 1, 2, 4, 8, 13, ㉖	26
			2	Pre, ⓪ 1, 2, 4, 8, ⑬, ㉖, ㊽	52
C	AAVrh.10Null	1.5×10^{12}	1	Pre, 0, 1	1
			1	Pre, 0, 1, 2, 4, 8, ⑬	13
			1	Pre, 0, 1, 2, 4, 8, 13, ㉖	26
			1	Pre, ⓪ 1, 2, 4, 8, ⑬, ㉖, ㊽	52
D	PBS	None	1	Pre, 0, 1	1
			1	Pre, 0, 1, 2, 4, 8, ⑬	13
			1	Pre, 0, 1, 2, 4, 8, 13, ㉖	26
			1	Pre, ⓪ 1, 2, 4, 8, ⑬, ㉖, ㊽	52
	Total		24		

The two doses of the test vector were chosen to bracket previously tested doses[14] and are equivalent to a weight adjusted human dose of 2.85×10^{11} and 1.5×10^{13} gc based on the ~ 10-fold smaller size of NHPs compared to humans. The vectors were bilaterally administered to three cortical white matter sites per hemisphere, each at two depths, based on results from experiments described previously.[14] For each sacrifice time point, AAVrh.10hARSA experiment groups consisted of $n = 2$ (1 male, 1 female), and control groups (AAVrh.10Null or PBS) consisted of $n = 1$ (male or female).

[a]At the indicated times, the NHPs underwent various assessments and sample collections as detailed in Table 2.

[b]To monitor changes in brain anatomy over time postsurgery and vector administration, CNS MRIs were performed for groups/time points indicated by black circles.

[c]At indicated time points necropsy was performed as detailed in Table 2.

AAV, adeno-associated virus; ARSA, arylsulfatase A; CNS, central nervous system; gc, genome copies; MRI, magnetic resonance imaging; NHPs, nonhuman primates; PBS, phosphate buffered saline.

without respect to weight or age, using a random number generation program (MS Excel). The surgical assistant maintained a spreadsheet of animal numbers (tattoos), cage numbers, vector vial lots, and treatments. All investigators were blinded to treatment status of the animals throughout the trial. Unlocking of the treatment key was done only at the end of the study before the preparation of the pathology report. The pathologist was blinded to the treatment during evaluation of gross pathology and histopathology and was later unblinded to interpret the results and to compile the report.

There were no incidents or severe adverse events noted during the course of the trial that required unlocking the treatment blind. The only adverse effects observed during the study were localized to the site of administration as identified by CNS MRI.

The trial design included two doses. The lower of the two doses of AAVrh.10hARSA (2.85×10^{10} gc; 2.4×10^9 gc/site, Group A) was chosen to be equivalent (adjusted for the difference in weight of average NHP and humans) to that used in our clinical trial for CLN2 disease using the same method of delivery (BB IND 13591). The higher dose was $\sim$500-fold higher (1.5×10^{12} gc; 1.3×10^{11} gc/site) and was tested for both AAVrh.10hARSA and the control, AAVrh.10Null (Groups B and C, respectively), and was chosen to match the dose used in our previous NHP biodistribution study.[14] The NHP administered with AAVrh.10hARSA or controls (AAVrh.10Null and PBS) was euthanized at 1 week (for acute toxicity) and at 13, 26, and 52 weeks (for chronic toxicity). At each sacrifice time point, AAVrh.10hARSA experiment groups consisted of two NHPs (one male/one female), while the control groups (AAVrh.10Null or PBS) consisted of one NHP, alternating male/female by time point.

All NHPs were assessed for immune (anti-AAVrh.10 antibody titers), clinical (behavior), hematological, and serum chemistry parameters at three to nine time points and brain histopathology at four end points (1, 13, 26, or 52 weeks; Table 1) postadministration. The 52-week long-term animals were assessed by MRI scans at four time points during the study (at weeks 0 [presurgery], 13, 26, and 52 [before necropsy]; Table 1 [black circles]). MRI scans were performed on 13- and 26-week animals, before necropsy, for safety monitoring. No additional MRI scans were performed on the 1-week animals ($n = 6$) (Table 1). In total, 18 of the 24 NHPs were monitored by MRI as part of the safety study for long-term effects of the vector dose and/or surgery-induced inflammation.

All NHPs in the study underwent the same surgical procedure and sterile administration of AAV vectors (AAVrh.10hARSA, AAVrh.10Null) or PBS to the white matter (centrum semiovale) at three sites in each hemisphere (two locations in the frontal lobe [anterior and posterior] and one in the parietal lobe; see Supplementary Fig. S1). The vector or PBS was distributed to the CNS in a total of 180 μL per NHP brain, divided equally among 12 loci (15 μL/site), delivered using the flexible fused silica catheter described previously,[14,19] through six burr holes, at two depths per burr hole (see Supplementary Data for details on the surgeries and vector administration). This delivery method was based on results from experiments described previously and is identical to the method used in our clinical study for CLN2 disease (FDA BB IND13591).

Health assessments

The NHPs were observed and monitored daily by experienced personnel for general appearance, signs of toxicity, distress, and changes in behavior. The animals were housed singly immediately following surgery for 1–3 days and paired for the rest of the time. Behavioral assessments were recorded with NHP in separate cages to minimize interference. At multiple time points, the NHPs were sedated for assessment of general safety parameters, including temperature, pulse, respiratory rate, and weight (Table 2). For the acute toxicity arm of the study (1 week), assessments were performed at >1 week before surgery, on the day of administration (0), and at 1 week (before necropsy). For the chronic toxicity arm of the study (13 to 52 weeks), assessments were performed at >1 week before surgery, on the day of administration (0), and based on necropsy time point, at 1, 2, 4, 8, 13, 26, and 52 weeks.

There were a maximum of seven assessments for the 13-week animals, eight for the 26-week animals, and nine assessments for the 52-week animals. Allowable time windows for assessment up to 2 weeks were ±1 day and times over 2 weeks were ±3 days. Following the general health assessment, the NHPs underwent venous blood sampling for serum chemistry and complete blood count (CBC) (Table 2). The analyses were performed on an IDEXX ProCyte Dx hematology analyzer and Beckman Coulter AU680 clinical chemistry analyzer by the Laboratory of Comparative Pathology (Memorial Sloan-Kettering Cancer Center, New York, NY) in a blinded manner. Blood smears were prepared and examined by experienced medical technologists to validate the automated results obtained by the hematology analyzer. The normal range for each blood parameter was calculated separately per sex as the mean ± 2 × standard deviations of that parameter of all monkeys in the study using the two presurgery time points.

Cerebrospinal fluid assessment

As an additional safety assessment of direct intraparenchymal administration of AAVrh.10hARSA, cerebrospinal fluid (CSF) was analyzed from each NHP at two time points: presurgery and at the study end point (1, 13, 26, or 52 weeks) for anti-AAV antibodies. CSF was obtained from either the cisterna magna or through lumbar (L4/L5) taps.[20,21] The position of the needle was confirmed by free flow of clear CSF back into the hub, with collection of $\sim$500 μL for analysis. The CSF was exam-

Table 2. *Design of the safety studies in nonhuman primates*

Parameter		Time of Assessment (Study Week)[a]							
	Pre	0	1	2	4	8	13	26	52
Vector/vehicle administration[b]		■							
Physical examination	■		■		■		■		■
Clinical observations	■	■	■	■	■	■	■	■	■
Weight, rectal temperature, vital signs[c]	■	■	■	■	■	■	■	■	■
Complete blood counts[d]	■	■	■	■	■	■	■	■	■
Serum chemistry[e]	■	■	■	■	■	■	■	■	■
CSF[f]		■	■				■	■	■
Anti-AAVrh.10 immunity[g]	■	■	■	■	■	■	■	■	■
Behavior[h]	■	■	■	■	■	■	■	■	■
MRI[i]	■						■	■	■
Sacrifice[j]			■				■	■	■
Gross and histopathology[k]			■				■	■	■

[a]$n = 24$ (13F/11M). Study day 0 was day of surgery; all observations and safety assessments on day 0 were performed before surgery. Times for assessment for remaining time points were as follows: up to 2 weeks acceptable timeframe was ±1 day and for times over 2 weeks it was ±3 days.

[b]Vector dosing: PBS ($n = 2$F/2M); AAVrh.10Null, 1.5×10^{12} gc ($n = 3$F/1M); AAVrh.10hARSA, 2.85×10^{10} gc ($n = 4$F/4M); AAVrh.10hARSA, 1.5×10^{12} gc ($n = 4$F/4M). A subset of each group was euthanized at 1, 13, 26, and 52 weeks as detailed in Table 1.

[c]Assessment of general safety parameters, including temperature, pulse, respiratory rate, and weight.

[d]Complete blood tests included: white cell count, red blood cell count, reticulocytes (% and absolute), hemoglobin, hematocrit, mean corpuscular volume, mean corpuscular hemoglobin, mean corpuscular hemoglobin concentration, segmented neutrophils (% and absolute), lymphocytes (% and absolute), monocytes (% and absolute), eosinophils (% and absolute), basophils (% and absolute), and platelet count.

[e]Serum chemistry tests included: alkaline phosphatase, alanine aminotransferase, aspartate aminotransferase, gamma glutamyl transferase, albumin, total protein, globulin, total bilirubin, BUN, creatine kinase, triglycerides, glucose, lactate dehydrogenase, calcium, phosphorus, bicarbonate, amylase, lipase, sodium, chloride, potassium, sodium/potassium, albumin/globulin, and BUN/creatinine ratios, anion gap.

[f]CSF was collected at two time points per NHP, before vector administration and at necropsy, for analysis (quantification of ARSA protein and anti-AAVrh.10 total and neutralizing antibodies).

[g]Assessments included: humoral anti-AAVrh.10 capsid immunity by serum total anti-AAVrh.10 and neutralizing AAVrh.10 antibody titers and by CSF total anti-AAVrh.10 titers and CSF neutralizing anti-AAVrh.10 antibody titers.

[h]At the indicated times, behavioral assessments were performed with videotaping at rest and in responses to a series of standardized challenges, with extraction of quantitative traits as previously described.

[i]MRI was performed on groups described in Table 1.

[j]A subset for each time point as described in Table 1.

[k]Before necropsy, blood and CSF were sampled for analyses as detailed in footnotes d to g. During the necropsy, the animals were observed for pathology, with organs weighed and examined for gross pathology and abnormalities. The brain was excised, divided into hemispheres, and fixed with 10% formalin for histopathology examination of the administration sites. Samples of other organs (liver, lung, biceps, kidney, gonads, seminal vesicles, testes, epididymides, skin, spleen, ileum, heart, multiple sections of the spinal cord, lymph nodes, eyes with lacrimal glands, optic nerve, glossopharyngeal nerve, facial nerve, parotid and submandibular salivary glands, and any gross abnormalities) were collected at necropsy, fixed with formalin for histopathological analysis.

■ = test required for the research study.

BUN, blood urea nitrogen; CSF, cerebrospinal fluid; F, female; M, male.

ined to ensure that there was no blood contamination, then centrifuged (3,000 rpm, 4°C, 10 min), aliquoted, and frozen at −80°C for testing.

Anti-AAV antibody titers

Blood samples at each time point and CSF at presurgery and necropsy time points were assessed for anti-AAV total and neutralizing antibody titers. Total anti-AAVrh.10 antibody titers in the blood and CSF were measured by an enzyme-linked immunosorbent assay.[17] Sera or CSF from NHP that had been treated with AAVrh.10hARSA, AAVrh.10Null, or PBS controls was twofold serially diluted and then added to each well. Anti-AAVrh.10 antibody titers were calculated by interpolation of the log(OD) versus −log(dilution) with a cutoff value equal to twofold the absorbance of background. AAVrh.10 neutralizing antibody titers were assessed for each blood and CSF samples by an *in vitro* assay performed in 96-well plates with 293-ORF6 cells. AAVrh.10Luc (10^9 gc) was incubated with serial dilutions of sera or CSF from AAVrh.10hARSA administered or control NHP. The neutralizing antibody titer was expressed as the reciprocal of serum/CSF dilution at which 50% inhibition of AAVrh.10Luc was observed.[17,22]

Behavioral assessments

The NHPs were monitored by a standard set of behavior parameters. Before sedation for blood draws, assessments were performed at >1 week before surgery (Pre), on the day of administration (0), and at 1, 2, 4, 8, 13, 26, and 52 weeks. Each NHP was visually assessed for behavioral changes by videotaping them in individual home cages. The sessions were videotaped for 3 min, in the absence of outside stimuli, to observe nonstimulated "normal" behavioral activity, without outside reinforcements. Behaviors were scored by observers ($n = 2$), who were blinded to treatment, from the video tape sessions. The animals were assessed for typical and atypical behaviors from five clinical categories (Supplementary Table S1) for number of times the NHP performed specific behaviors, scoring "1" for 5 s of each behavior. The sum of normal behaviors (anxiety, arousal, and quiet behavior categories) was cal-

culated as the "Healthy" score (defined in Supplementary Table S1); and the sum of abnormal behaviors (sedation and abnormal motion categories) was calculated as the "Abnormal" score for each session. The normal behaviors were assessed based on a previous data set.[14,16–18]

Brain MRI

All imaging data were acquired on a 3.0 Tesla Siemens TIM TRIO MRI scanner (Siemens Healthineers, Erlangen, Germany) using a single channel loop resonator. The three-dimensional (3D) T_1-Weighted Magnetization Prepared Rapid Acquisition Gradient Echo scan was acquired using a: 2,300 ms repetition time, 1,100 ms inversion time, 3.4 ms echo time, 8° flip angle, $0.5 \times 0.5 \times 0.5$ mm resolution with a 19.2 cm field of view, and a 384×384 matrix. The 52-week NHPs were monitored using CNS MRI at four time points (presurgery, 13, 26, and 52 weeks [before necropsy], ±6 days). Additional MRI scans were performed on 13- and 26-week animals in each dose cohort, once before necropsy. No acute 1-week animals were assessed by MRI. The MR technologist was blinded to treatment.

The coronal 3DT1 images were analyzed using ImageJ (version 1.52; National Institute of Health) to identify regions of interest (ROIs) in the NHP brains. ROIs were traced and the area (mm^2) measured using ImageJ software version 1.52a (Wayne Rasband; NIH, Bethesda, MD). The area for each ROI was determined across multiple coronal slices and the lesion volume calculated. The 3D volume of the NHP brain was determined using AFNI software (Robert Cox; NIMH, Bethesda, MA). The 3dSkullStrip command with surface coil and primate corrections was used to strip the skull from the MRI images. The volume of the resulting skull stripped brain was calculated by converting the total number of voxels to milliliter. The volume of the abnormality was then normalized to the total brain volume and presented as a percentage.

Necropsy

Each dose cohort included NHP euthanized at 1 week ±1 day (for acute toxicity) and at 13, 26, and 52 weeks ±3 days (for chronic toxicity). Before euthanasia, safety assessments were performed on all NHPs (behavior, weight/vitals, blood, and CSF sampling) as described above. All NHPs in the chronic toxicity time points (13, 26, and 52 weeks) had additional MRI brain scans performed. At sacrifice, euthanasia was carried out with intravenous sodium pentobarbital (Euthasol, Virbac, Westlake, TX), and the animal death confirmed by the loss of corneal reflexes. The animals were perfused through cardiac puncture with cold PBS followed by complete necropsy (gross examination, organ weights, and sample collection for histopathology). All organs were examined grossly during necropsy performed by a board-certified veterinary pathologist, and gross findings were recorded.

The brain was excised from the skull, weighed, and divided into two hemispheres for analysis. The left hemisphere was fixed in 10% neutral buffered formalin for 2 weeks, then sectioned into 3 mm coronal sections for histopathology, all sections were photographed and any gross findings were noted, and multiple sections especially those around the administration sites were sampled and processed for histopathology and immunohistochemistry (IHC). The right hemisphere was processed during necropsy by sectioning into 1 cm coronal slabs, flash frozen in liquid nitrogen, and stored at −80°C for later assessment. The spinal cord was extracted at three levels from each NHP: cervical C3–C4, thoracic T6–T7, and lumbar L2–L4 and placed in 10% neutral buffered formalin for histopathology and IHC.

Sections of organs collected at necropsy were processed routinely in alcohol and xylene, embedded in paraffin, sectioned at a 5 μm thickness, stained with hematoxylin and eosin (H&E), and examined by a board-certified veterinary pathologist, who evaluated the slides in a blinded manner and interpreted the combined anatomic pathology (macroscopic and microscopic postmortem examination) data. Additional sections of the CNS were prepared from sites of administration and sections that were determined to be 1 cm distal (caudal) for comparison for each NHP in the study and stained by IHC for cell markers (CD3, CD20, and CD68) to assess infiltration by lymphocytes, microgliosis, and monocyte-derived macrophages (see Supplementary Data for details).

After the slide interpretation was completed, the pathologist was unblinded to treatment and interpreted the gross findings, histopathology, hematology, and serum chemistry results in the context of the experimental history and in-life observations. Findings were determined to be treatment related or not, and adverse or not, by the pathologist following standard guidelines for preclinical safety studies.[23] As a final step, the pathologist of record prepared a report comparing the toxicology of the test article in the two dose groups versus control NHP.

Statistical analyses

All statistical analyses were performed with GraphPad Prism v6.02 (GraphPad Software, San Diego, CA). Statistical analyses comparing the different cohorts to PBS-treated controls were generated using one-way analysis of variance (ANOVA) with Dunnett's multiple comparison test and for NHP behavior by two-way repeated measures of ANOVA (RM-ANOVA) with Dunnett's multiple comparison test. Values that were at least $p < 0.05$ were considered significant. Evaluations of blood counts and serum chemistries were performed by a two-tailed paired t-test at various time points to identify significant differences due to time ("aging"). Post-test *Ad hoc* analysis was performed with Tukey's multiple comparison test for RM-ANOVA results displaying significance. Due to daily

variations in cell numbers and serum chemistries in sample sizes $n < 5$ per gender, the significance level was set at $p < 0.01$ to increase the statistical power for these parameters and to screen for outliers.[15,16,24,25]

RESULTS
General safety and clinical observations

No acute or adverse side effects were noted by the blinded observers during daily/weekly observation evaluations. No unscheduled mortality or clinical abnormalities attributed to treatment were observed during the 1 year study. At a clinical level, the vector was well tolerated by the animals at both vector dosages.

There were no vector-associated adverse clinical signs observed through the length of the study. There were no significant differences in body weights in the low- and high-dose groups compared with the PBS-administered control group during the course of the study (Supplementary Fig. S2). There were no significant differences in vitals (heart rate, respiratory rate, and body temperature) in the vector dosage groups compared to the PBS controls (not shown).

Serum chemistry and hematology assessments

Animals were evaluated for an extensive set of serum chemistry and hematologic toxicology parameters at nine time points over the 1 year study (Supplementary Figs. S3 and S4). No serum chemistry or hematology changes attributed to the test articles were observed. The liver and muscle enzymes (alanine aminotransferase [ALT], aspartate aminotransferase, lactate dehydrogenase, and creatine kinase) were mildly elevated at the 1-week postsurgery time point in most animal samples for all treatment groups in both genders (Supplementary Fig. S3E–G, U). This was not unexpected and is frequently observed, including in our previous NHP studies, and is attributed to transient muscle injury in animals undergoing surgery with anesthesia.[14,17,26] The elevated levels returned to the normal range by the next time point (2 weeks) in most cases, except for a couple of outliers for ALT serum levels. These increases were not considered adverse as it was an expected postsurgical change and restored to normal levels.

Sporadic changes of hematologic parameters were observed in single animals or small numbers of animals at several time points of the study (Supplementary Fig. S4). These values were occasionally outside of reference ranges; however, these sporadic changes did not constitute trends, did not appear to be associated with treatment groups, or correlate with clinical abnormalities or gross or microscopic pathologic findings. These blood parameter changes were considered to represent normal occurring variations. No significant correlations were observed between treated groups and the control groups nor were the means of data from the treated cohorts outside the normal range of pretreatment levels (gray shaded areas in Supplementary Figs. S3 and S4) in the serum chemistry or hematologic assessments.

Immunity against AAVrh.10

No NHP had detectable anti-AAVrh.10 total or neutralizing antibodies pretherapy. As expected, after treatment, the titer of anti-AAVrh.10 total and neutralizing antibody increased in a dose-dependent manner. Analysis of serum collected at multiple time points demonstrated that administration of AAVrh.10hARSA by intraparenchymal routes was associated with the development of anti-AAVrh.10 antibodies (Fig. 1A–D). The development of antivector titers was dose dependent but not gender specific, unlike that observed in mice.[22,27,28] Total anti-AAVrh.10 antibody titers peaked at 13 weeks for most animals, remaining high for the length of the study in animals from the high-dose cohort but decreased for three animals in the low-dose cohort, reaching titers comparable with the PBS controls (Fig. 1A, B).

As expected, the dose-dependent anti-AAVrh.10 neutralizing antibody titers were one to three logs lower than the total anti-AAVrh.10 serum antibody titer (Fig. 1C, D). For most NHPs, the neutralizing titers remained persistent over the period of observation, with similar patterns in males versus females. Comparison of neutralizing versus total antibody titers demonstrated, for both males and females, that detectable neutralizing titers were observed with $>10^3$ total anti-AAVrh.10 titers (Fig. 1E, F).

Total anti-AAVrh.10 antibody levels were observed in the CSF of NHP in the high dose cohorts (AAVrh.10-hARSA and AAVrh.10Null), but not in the low dose (AAVrh.10hARSA) or PBS control groups (Fig. 2A–D). Comparisons between the serum and CSF anti-AAVrh.10 titers failed to show correlation (Fig. 2E–H). Only one NHP (high dose AAVrh.10hARSA, female) out of the 24 NHPs tested had a positive neutralizing titer above assay background (Fig. 2C). The same NHP had the highest CSF total anti-AAVrh.10 titers (Fig. 2A), suggesting that total CSF antibody titers need to be above 10^4 before neutralizing titers are observed in the CSF.

Assessment of NHP behavior

The behavior of the NHP was assessed at nine time points over the course of the study. Blinded videotape analysis by multiple observers of NHP behavior presurgery and postadministration showed no discernible neurological differences in any of the vectors or doses tested (Supplementary Fig. S5). All NHP scores of "healthy" activities (Supplementary Table S1) were within the historic range of normal NHP behavior, as calculated from presurgery data (Supplementary Fig. S5A, B). The treatments did not increase hyperactivity nor provoke somnolent episodes in the animals. No difference was seen
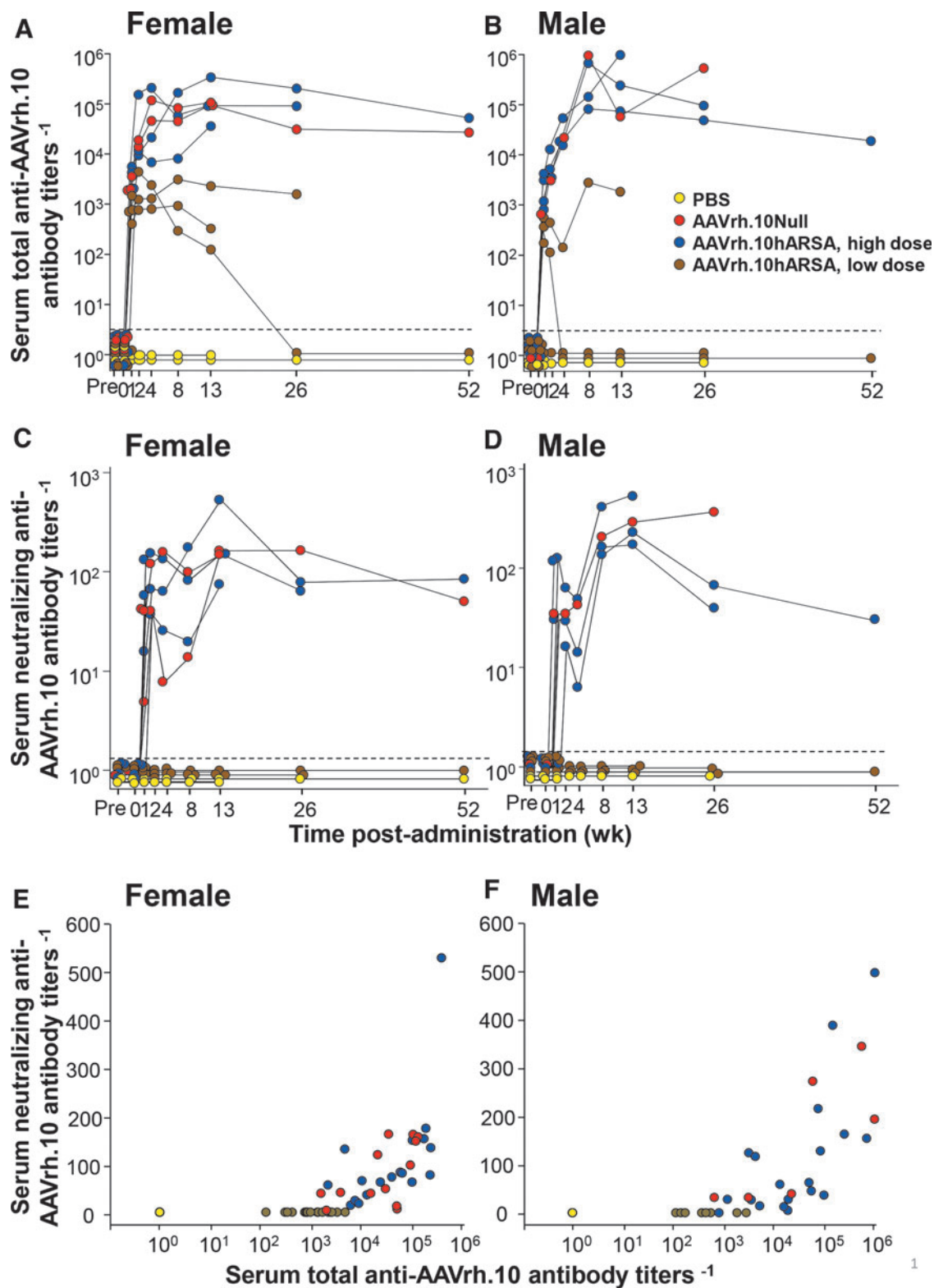
Figure 1. Assessment of serum total and neutralizing anti-AAVrh.10 antibody titers evoked by administration of AAVrh.10hARSA. Total anti-AAVrh.10 antibody and neutralizing anti-AAVrh.10 antibody titers in the NHP serum were determined over time, after intraparenchymal administration of AAVrh.10hARSA (low dose 2.85×10^{10} gc, 2.4×10^9 gc/site or high dose 1.5×10^{12} gc, 1.3×10^{11} gc/site), AAVrh.10Null, or PBS. The total antibody titer is expressed as the reciprocal of the serum dilution. The neutralizing antibody titer is expressed as the reciprocal of serum dilution at which 50% inhibition of AAVrh.10Luc was observed. Shown are the results for each NHP in the study, color-coded by treatment (*yellow*, PBS; *red*, AAVrh.10Null; *blue*, AAVrh.10hARSA-high dose; brown, AAVrh.10hARSA-low dose). **(A, B)** Total serum antibody titers. **(C, D)** Neutralizing antibody titers. **(A, C)** Females ($n = 13$); **(B, D)** Males ($n = 11$). A subset of each group was euthanized for histopathology at 1, 13, 26, and 52 weeks, and therefore, the number of individual assessments decreased with time. Assay LOD was 10^0; any sample results below the LOD were recorded as 1 by convention. Background of both assays was 2.0, as represented by the *black dashed line*. **(E, F)** Comparison of neutralizing to total anti-AAVrh.10 titers evoked by administration of AAVrh.10hARSA. The data in **(E, F)** were compared as neutralizing anti-AAVrh.10 antibody titers versus total anti-AAVrh.10 antibody titers for each corresponding each time point. **(E)** Female **(A** vs. **C)**; **(F)** Males **(B** vs. **D)**. AAV, adeno-associated virus; ARSA, arylsulfatase A; gc, genome copies; LOD, limit of detection; NHP, nonhuman primate; PBS, phosphate buffered saline.
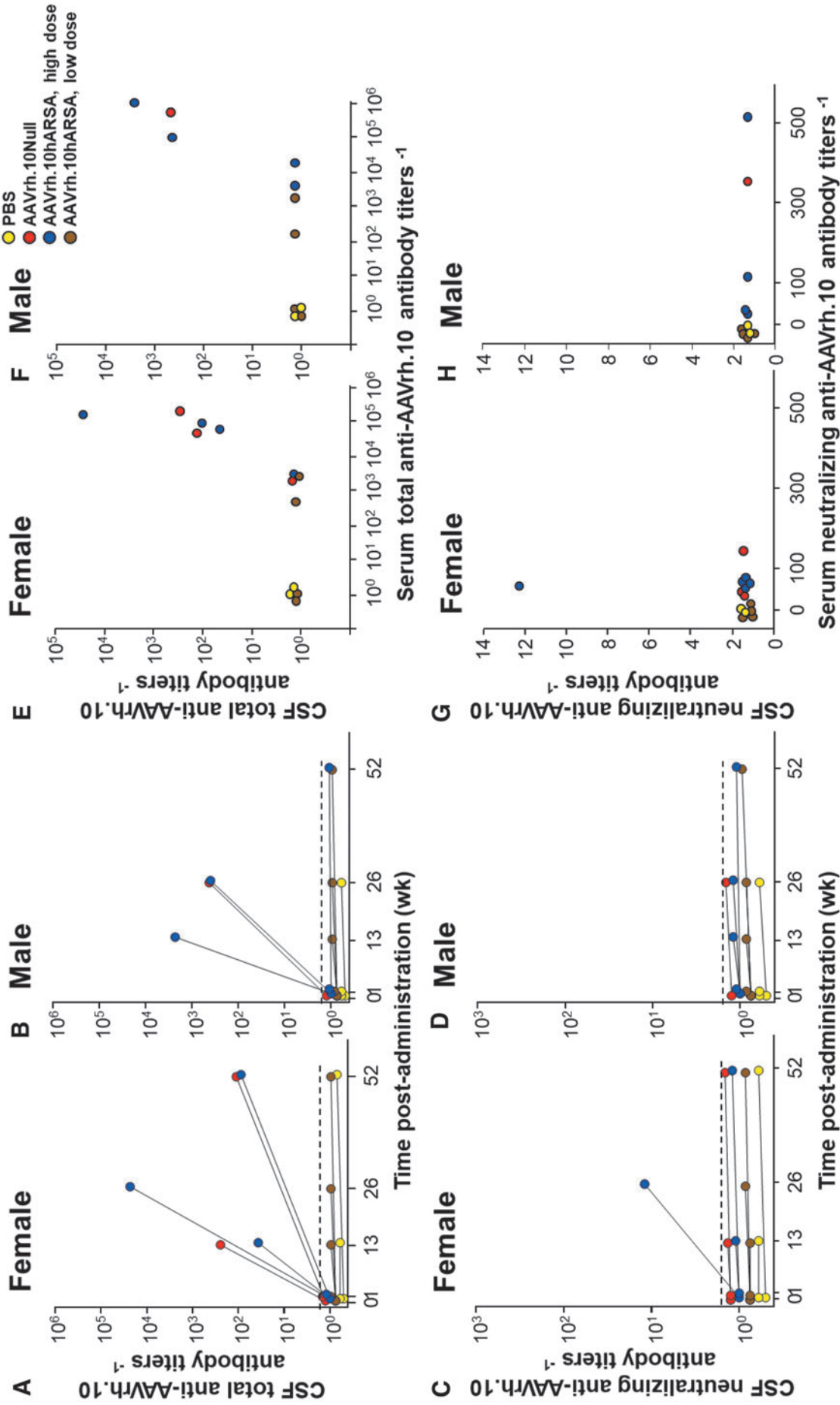
Figure 2. Assessment of total and neutralizing anti-AAVrh.10 antibody titers in NHP CSF for humoral responses evoked by administration of AAVrh.10hARSA. Total anti-AAVrh.10 antibody and neutralizing anti-AAVrh.10 antibody titers in the CSF were determined after intraparenchymal administration of AAVrh.10hARSA (low dose 2.85×10^{10} gc, 2.4×10^{9} gc/site or high dose 1.5×10^{12} gc, 1.3×10^{11} gc/site), AAVrh.10Null, or PBS at two time points, before vector administration (day 0) and before necropsy (at 1, 13, 26, or 52 weeks). At indicated time, the NHPs were sedated for sampling of CSF using cisterna magna with assessment of antibody titers in CSF. The total antibody titers are expressed as the reciprocal of serum dilution at which 50% inhibition of AAVrh.10Luc was observed. Shown are the results for each NHP in the study, color-coded by treatment (*yellow*, PBS; *red*, AAVrh.10Null; *blue*, AAVrh.10hARSA-high dose; *brown*, AAVrh.10hARSA-low dose). **(A, B)** Total CSF antibody titers. **(C, D)** Neutralizing antibody titers. **(A, C)** Females ($n=13$); **(B, D)** Males ($n=11$). The day 0 and necropsy CSF values are connected for individual NHP. Assay LOD was 10^{0}; any sample results below the LOD were recorded as 1 by convention. Background of the assay was 2.0, as represented by the *dashed line*. **(E, F)** Comparison of CSF total to serum total anti-AAVrh.10 antibody titers evoked by administration of AAVrh.10hARSA. The data in Figures 1A, B and **(A, B)** were compared as CSF total anti-AAVrh.10 antibody titers versus serum total anti-AAVrh.10 antibody titers for each corresponding each time point. **(E)** Female (Fig. 1A vs. **A**); **(F)** Males (Fig. 1B vs. **B**). **(G, H)** Comparison of CSF neutralizing anti-AAVrh.10 titers to serum anti-AAVrh.10 neutralizing titers. The data in Figures 1C, D and **(C, D)** were compared as CSF neutralizing anti-AAVrh.10 antibody titers versus serum neutralizing anti-AAVrh.10 antibody titers for each corresponding each time point. **(G)** Female (1C vs. **C**); **(H)** Males (1D vs. **D**). CSF, cerebrospinal fluid.

between the PBS versus AAV-treated NHP for males or females (one-way ANOVA with Bonferroni's multiple comparison test): PBS versus high dose AAVrh.10hARSA, $p > 0.9$; PBS versus low dose AAVrh.10hARSA, $p > 0.3$; PBS versus high dose AAVrh.10Null, $p > 0.9$; overall $p > 0.3$. No adverse effects (such as sedation or dyskinesia, Supplementary Table S1) were observed other than two NHPs displaying stereotypy (scratching and pacing), at both pre- and postsurgery time points. No NHPs in the four cohorts displayed any abnormal deficits (head tilts, comatose, or altered levels of consciousness) at any time postsurgery and vector administration.

MRI assessment

For a subset of the NHPs ($n = 6$, 52 weeks cohort), the brains were monitored using MRI at presurgery and at 13, 26, and 52 weeks postsurgery/vector administration and compared to brain scans of a PBS-treated NHP (Fig. 3). For the remaining animals, NHP in each dosage group received MRI at 13 or 26 weeks before their preassigned necropsy time point. In the majority of the NHPs assessed by MRI, a thin line surrounding the catheter insertion and the site of vector administration in the parenchyma could be observed (Fig. 3, AAVrh.10hARSA panels, yellow arrows). In the 3/3 long-term control NHP administered
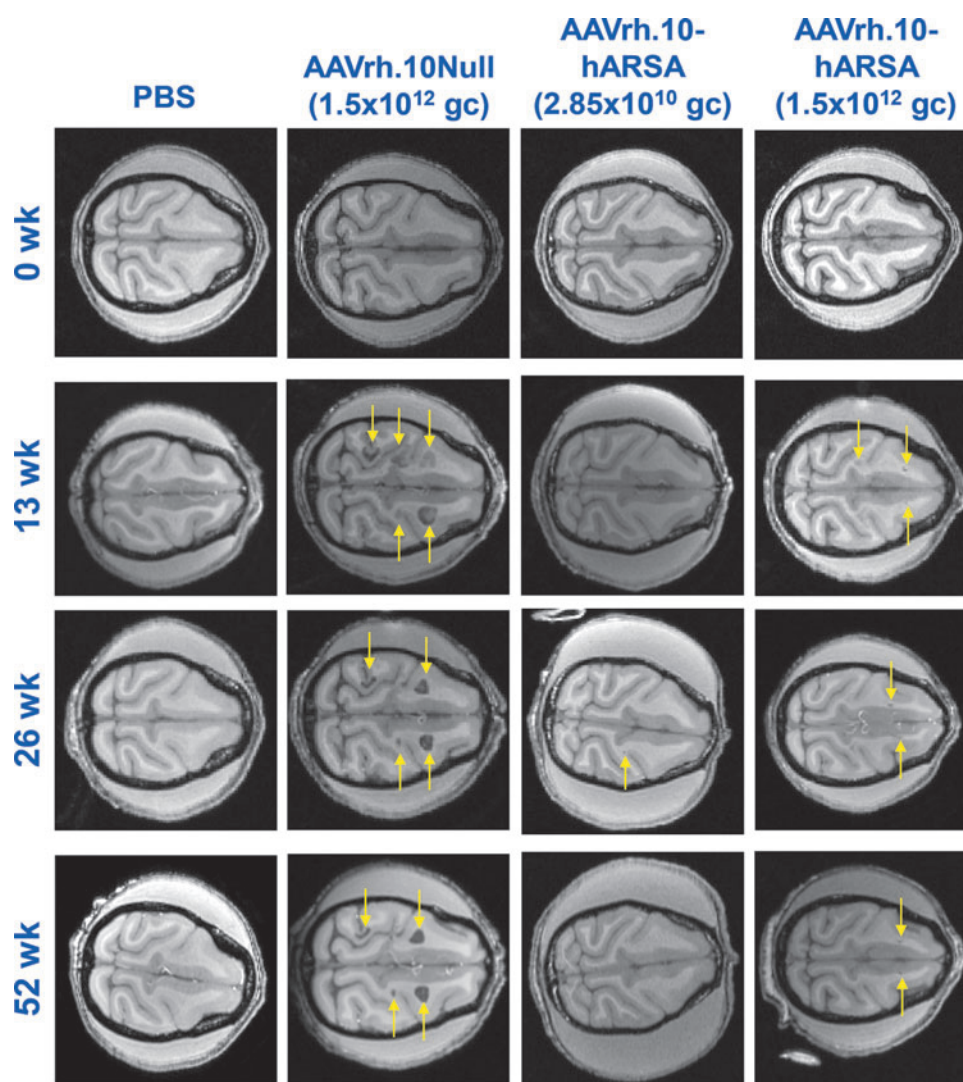

Figure 3. CNS MRI assessment following CNS administration of AAVrh.10hARSA to NHPs. NHP in the long-term studies (52 weeks, $n = 6$; 4 female/2 male) were analyzed by T1 weighted MRI scans at 0, 13, 26, and 52 weeks after intraparenchymal administration of the AAVrh.10hARSA vector (2.85×10^{10} gc, 2.4×10^9 gc/site or 1.5×10^{12} gc, 1.3×10^{11} gc/site) or the AAVrh.10Null vector (1.5×10^{12} gc) or PBS. Times for assessment were ± 6 days. Shown are axial slices (0.5 mm thick) of the head from the same NHP at specific time points. The depth of the axial slice displayed is 1.0 cm from superior aspect of brain; the same sections were matched between animals for the image scans. The first *column* (*far-left*) contains images from PBS group NHP (female); second *column* (*left*), AAVrh.10Null-treated NHP (female); third *column* (*right*), low dose AAVrh.10hARSA-treated NHP (male); and fourth *column* (*far-right*), high dose AAVrh.10hARSA-treated NHP (female). The rows contain images for each assessment time point (0, 13, 26, and 52 weeks). Orientation of the MRI scans of the NHP heads is posterior (*left*) to anterior (*right*), with the longitudinal fissure, horizontal in the panels. The *yellow arrows* denote ROIs, including pathologic findings in the T1 scans. These findings were confirmed on T2 and T2-FLAIR scans (not shown) during the same imaging session. CNS, central nervous system; MRI, magnetic resonance imaging; ROIs, regions of interest.

the AAVrh.10Null vector, abnormal ROIs >0.5 cm in size were detected in the MRI scans beginning at 13 weeks (Fig. 3, AAVrh.10Null panels, yellow arrows). All three NHPs presenting with abnormal MRI findings received the same lot of AAVrh.10Null control vector.

No such abnormalities were observed with the AAVrh.10hARSA vector, at either dosage. Small faint gray ROIs were noted on scans in two of the six high dose AAVrh.10hARSA cohorts (examples shown in Fig. 3). The MRI ROIs for all NHPs were subsequently quantified on each MRI series and calculated as ''% of total brain volume'' (Supplementary Fig. S6A, B). These areas remained the same size at each MRI session with reduction in one NHP (Fig. 3 and Supplementary Fig. S6). These findings were confirmed on T2 and T2-FLAIR scans (not shown) performed during the same imaging session. Comparisons of the treatment groups for overall effect of treatment on MRI abnormalities showed significant differences between the AAVrh.10Null cohort and the AAVrh.10hARSA treatment cohorts, $p < 0.0001$ (AAVrh.10Null vs. AAVrh.10hARSA, high dose), $p < 0.0001$ (AAVrh.10Null vs. AAVrh.10hARSA, low dose), $p < 0.0001$ (AAVrh.10Null vs. PBS), $p < 0.02$ (AAVrh.10hARSA, high dose vs. AAVrh.10hARSA, low dose; Supplementary Fig. S6B).

The presence of MRI abnormalities in the NHPs that received AAVrh.10Null led us to reevaluate the vector lot quality control assay results for all vectors used in the study, to assess if these abnormalities were related in any way to a product impurity. The panel of product viability and safety parameters tested before lot release for use in toxicology studies included a bacterial endotoxin test (limulus amebocyte lysate), which reacts with endotoxin lipopolysaccharide from gram negative bacteria. The endotoxin level of the lot of AAVrh.10Null vector used for the negative control NHP was 4.04 EU/mL. This was within the Good Manufacturing Practice (GMP) specification of less than 20 EU/mL on the lot release, but it was higher than all other lots tested of AAVrh.10 vector used in the trial (0.05–0.5 EU/mL). It is possible that this higher level of endotoxin in the AAVrh.10Null vector lot contributed to the catheter tip local abnormalities detected on the MRI and the histopathology described below.

Gross pathology and organ weights

Pathologic observations during the necropsy documented no significant gross abnormalities and none that was attributed to the test articles in any of the dosage groups, except for those observed grossly on sectioning of the brain. In the PBS control and AAVrh.10hARSA low dose groups, examination of vector administration sites revealed small foci of brown discoloration of brain tissue that did not significantly differ in size or nature between these two groups. In the AAVrh.10hARSA high dose group, examination of these sites revealed similar but larger foci of brown discoloration, while in the AAVrh.10-

Null group, the pathology tended to be larger and some pathologic findings were accompanied by small, focal fluid filled cavitations of the brain tissue which corresponded to the pathologic findings observed on MRI. No significant differences in organ weights (absolute weights, organ/body and organ/brain weight ratios)[29,30] were observed between treated and control groups (not shown).

Histopathology

Histopathology was performed on multiple organs for each NHP (Supplementary Table S2), with assessment by the study pathologist, initially blinded to treatment and dose. Outside of the CNS, analysis of the organs did not reveal any abnormalities attributable to the AAVrh.10ARSA. Various minor findings were observed and were consistent with normally occurring incidental changes known to occur in NHPs or were attributed to experimental manipulations other than administration of the test article, such as anesthesia and surgery. Following the detection of abnormal ROIs in the MRI in-life scans, further histopathology assessments were carried out on the brains of these animals and matched controls by H&E (examples are shown in Fig. 4) and by staining for IHC cell markers (CD68 [activated macrophages], CD3 [T cells], and CD20 [B cells]), at the site of vector deposits and areas >1 cm distal to deposit sites (examples are shown in Fig. 5). The findings are summarized below for each study group.

PBS group.   Pathologic changes observed at the injection sites included focal pathology findings observed in the white and gray matter (see Table 3 for further details). The abnormal findings tended to have a linear shape perpendicular to the surface of the brain (Fig. 4A, B), compatible with the catheter tract, and were characterized by mild-to-moderate microglial or macrophage infiltrates (CD68$^+$ cells) and minimal T cell infiltrates (CD3$^+$). No B cells (CD20$^+$) were observed at the injection sites of the PBS group (Fig. 5A–F). Some of these focal pathology findings also displayed minimal-to-mild spongiosis of the neuropil. The pathology findings observed in this group are compatible with a reaction to the minor focal traumatic injury caused by the administration of PBS or surgery.

Low dose AAVrh.10hARSA group.   Pathologic changes were observed in the brain administration sites examined for this group of NHPs, with localized inflammatory pathologic findings that were similar in nature and size to the pathologic findings observed in the PBS group (Fig. 4E, F; Table 3). The pathologic findings included accumulation of T cells (minimal to mild, compared to minimal in PBS group) and contained minimal-to-mild B cell infiltrates, a finding not observed in the PBS group (Fig. 5M–R). These minimal-to-mild T and B cell infiltrates at the site of injection likely represent a mild immune reaction caused by the presence of AAVrh.10 and/
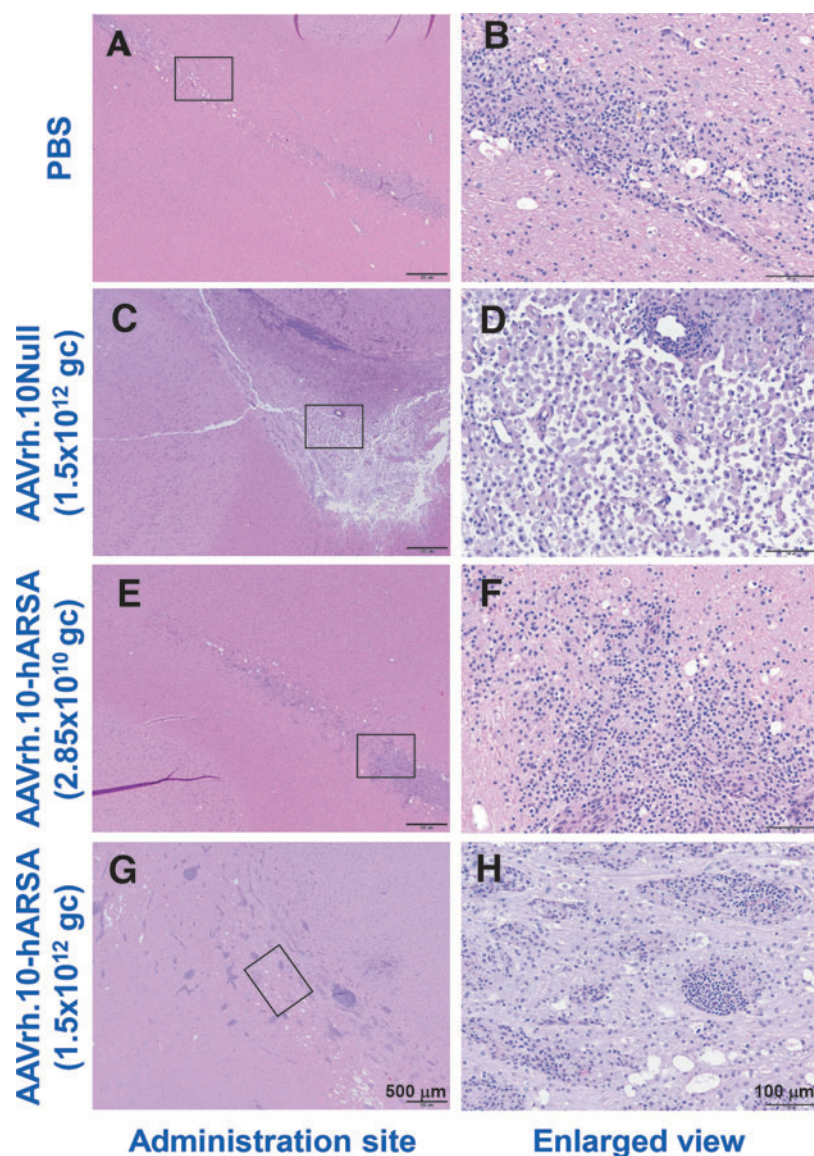
Figure 4. Histopathology assessment of the localized vector administration sites of AAVrh.10hARSA, AAVrh.10Null, and PBS in CNS. Shown is the histopathology of the brain coronal sections following necropsy of 1, 13, and 26 weeks NHP of the localized T1 MRI pathologic findings at the catheter sites. The coronal sections were stained with H&E. Examples of the findings are shown, with enlarged areas (*black boxes* in *left panels*) shown in the *right column*. The resulting brain pathology staining is shown for the PBS (male, 1 week, CNS site B; **A, B)**, AAVrh.10Null (female, 13 weeks, CNS site A; **C, D)**, low dose (male, 1 week, CNS site B; **E, F)**, and high dose (female, 26 weeks, CNS site A; **G, H)** AAVrh.10hARSA groups. Black scale bars = 500 and 100 μm. H&E, hematoxylin and eosin.

or human ARSA. This finding was minimal, focal, and not associated with any clinical abnormalities, and it was reversible as noted in the two animals euthanized at 52 weeks in this group. In the 52-week animals, no B cells were observed, and the number of T cells observed was minimal and indistinguishable from those of the PBS group.

High dose AAVrh.10hARSA group. For this dose group, the clinical pathologic findings at the injection sites in the acute 1 week NHP were generally similar to those observed in the low dose AAVrh.10hARSA group. However, in NHPs euthanized at weeks 13, 26, and 52, the sites of

vector administration (catheter tip; Fig. 4G, H and Table 3) had larger pathologic findings (up to 10.0 × 7.5 mm) and had moderate to marked T and B cell infiltrates with prominent perivascular cuffing. Gliosis and microglial/macrophages infiltrates were also marked in some pathologic findings (Fig. 5S–X). This increase in lesion size, T and B cell infiltrate, and microglial/macrophage infiltrate was dose dependent. These pathologic findings were not reversible as they were observed at week 52. However, the inflammatory infiltrates were localized and not observed at 1 cm distal to the pathologic findings surrounding the injection sites (Fig. 5T, V, X). No clinical abnormalities were observed in these animals.
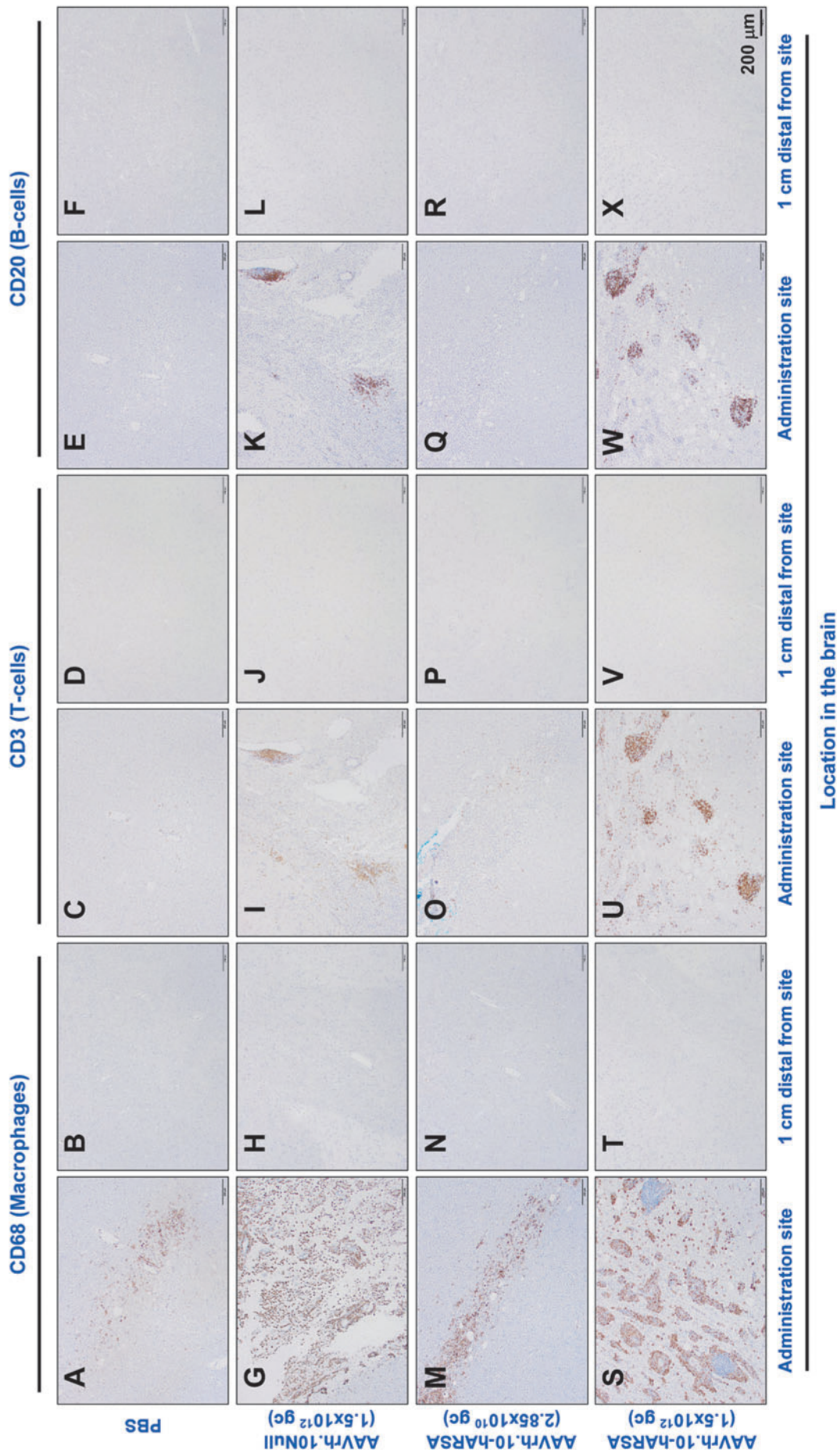
Figure 5. IHC assessment of inflammatory cells at the sites of administration of AAVrh.10hARSA, AAVrh.10Null, and PBS. Staining of the brain coronal sections from 1, 13, and 26 weeks NHP was done to assess the MRI ROIs and microscopic findings of concern to identify the types of inflammatory cells. The slides were stained by IHC for CD68 (microglial cells and monocyte-derived macrophages), CD3 (T cells), and CD20 (B cells). The resulting brain immunohistochemical staining is shown for the vector administration site and 1 cm distal from the administered site for PBS **(A–F)**, AAVrh.10Null **(G–L)**, low dose **(M–R)**, and high dose **(S–X)** AAVrh.10hARSA groups. Black scale bar = 200 μm. IHC, immunohistochemistry.

Table 3. *Summary of central nervous system histologic analysis*

		CNS Findings					
Vector	Total Dose (gc)	Pathologic Findings Observed	Areas of Pathology Changes[a]	Extent of Inflammatory Cell Accumulation[b]	Rever-sible[c]	Surgery Related?[d]	Vector-Related[e]
AAVrh.10hARSA	2.85×10^{10}	14 of 24 sites	0.2×0.1–6.5×0.6 mm[f]	Minimal to mild	Yes	No	Yes
AAVrh.10hARSA	1.5×10^{12}	22 of 24 sites	1.4×0.1–10.0×7.5 mm[g]	Moderate to marked	No	No	Yes
AAVrh.10Null	1.5×10^{12}	12 of 12 sites	3.2×0.2–13.3×7.3 mm[h]	Moderate to marked	No	No	Yes
PBS	None	4 of 12 sites	0.1×0.1–6.8×0.4 mm[i]	Minimal to mild	Yes	Yes	No

The term "pathologic finding" refers to any pathologic change observed by the pathologist in the tissues on gross or histologic examination, representing the direct effect or an insult and/or the tissue response to the insult, such as an immune response to the AAV capsid, ARSA transgene, or mechanical trauma from surgery. For each clinical pathology parameter examined, a standard three step approach was used to analyze the results to determine if an adverse effect caused by the test article was present.[23] (1) Is a significant difference observed between treated groups and the control group? (2) Does this difference represent an effect caused by the test article? (3) Is this effect considered to be adverse? Decisions 2 and 3 were made based on a weight of evidence approach based, in part, on discriminating factors described by Lewis *et al.*[23] Pathologic findings detailed for the CNS within this study are summarized in Table 3.

[a]Areas of pathology observed during pathologic examination of the CNS section slides of the vector administration sites are listed as the minimum to the maximum areas for the dosage cohort as measured (in mm) in the hematoxylin and eosin slides. See Fig. 6 for examples.

[b]Immunohistochemical staining of the CNS sites for extent of inflammatory cell accumulation was performed with anti-CD68 (for activated microglial/macrophages), anti-CD3 (for T cells), and anti-CD20 (for B cells) to assess infiltrate cell number and types in the lesion areas. Infiltrate categorizations are based on standard pathology scoring: Minimal (rare positive cells); mild (small number of positive cells); moderate (moderate number of positive cells); and marked (high number of positive cells). See Fig. 7 for examples.

[c]Reversible. As determined by the Pathologist of record whether the pathologic findings disappear over time, based on NHP necropsy for the 13-, 26-, or 52-week time points.

[d]Surgery-related. "Is the pathology attributed to surgery and mechanical trauma of the catheters and needles?"

[e]Vector-related. "Is the pathology attributed to the test article (AAVrh.10hARSA) as opposed to surgery?"

[f]Pathologic findings in the low dose group were generally similar in nature and size to the pathologic findings observed in the PBS group.

[g]Pathologic findings in the high dose group were significantly different from those of the low dose AAVrh.10hARSA group: they were larger with inflammatory infiltrates of T and B cells, which were forming prominent perivascular cuffs.

[h]Pathologic findings in the AAVrh.10Null vector control brains were generally similar to the high dose group with T and B cell and microglial/macrophage infiltrates, but they tended to be larger and most contained a large central zone of loss of brain tissue.

[i]Pathologic findings were observed in the white matter, gray matter, or leptomeninges, were focal, and often had a linear shape perpendicular to the surface of the brain, compatible with a needle tract.

AAVrh.10Null group. For this group of NHPs, receiving the control vector, the acute 1 week pathologic findings were similar to those observed in the high dose AAVrh.10hARSA group (Table 3). At weeks 13, 26, and 52, the injection site pathologic findings were generally similar to the high dose AAVrh.10hARSA group in their T cell, B cell, and microglial/macrophage infiltrates, but the pathology area tended to be larger and most pathologic findings contained a large central zone of loss of brain tissue, resulting in fluid filled cavitations (Figs. 4C, D, and 5G–L). The moderate to marked T cell, B cell, and microglial/macrophage infiltrates were similar to the pathologic findings of the high dose AAVrh.10hARSA group.

The increase in the size of the pathologic findings compared to the same dose of AAVrh.10hARSA (high dose group), as well as loss of brain tissue with cavitation, was not observed in any other treatment group. The increased lesion size and cavitation in the AAVrh.10Null group was interpreted as possibly related to the presence of a higher level of endotoxin in the vector preparation. These pathologic findings were persistent and were observed at week 52. No overt clinical abnormalities were observed in these animals during the in-life phase of the study.

Cervical, thoracic, and lumbar spinal cord

The spinal cord was examined for each NHP at each of three levels: cervical, thoracic, and lumbar. Examinations of the PBS ($n = 4$, 12 sections) and low dose AAVrh.10-hARSA ($n = 8$ animals, 24 sections) groups revealed no pathology in any spinal cord segments by H&E staining in 12 of 12 sections and 24 of 24 sections examined for PBS and low dose (2.85×10^{12} gc) AAVrh.10hARSA cohorts, respectively (cervical cord examples in Supplementary Fig. S7A, C). In contrast, the AAVrh.10Null ($n = 4$, 12 sections) and high dose AAVrh.10hARSA cohort ($n = 8$ animals, 24 sections) NHP cervical, thoracic, and lumbar spinal cord segments exhibited minimal-to-mild axonal degeneration and/or minimal gliosis in 4 of 12 sections and 5 of 24 sections examined for the AAVrh.10Null (1.5×10^{12} gc) and high dose AAVrh.10hARSA (1.5×10^{12} gc) cohorts, respectively, representing 2/4 animals in the high dose null group and 4/8 animals in the high dose ARSA group.

No pathology was detected in the 1 week acute animals for either of the high dose vector cohorts, but pathology was observed in the >13 weeks animals. These changes located in the white matter lateral funiculi of the spinal cords were unilateral or bilateral, with detection of dilated myelin sheaths and macrophages. One female 13 weeks high dose AAVrh.10Null animal showed minor pathology in all three cord samples tested; whereas the other animals only displayed mild to minor white matter pathology in the cervical region samples (examples in Supplementary Fig. S7B, D). While the pathologic findings were mild, they were not reversible and were observed at week 52 for both high dose (1.5×10^{12} gc) groups.

DISCUSSION

MLD is a fatal pediatric disorder with no approved therapy. The leukodystrophy is the result of a deficiency of lysosomal enzyme ARSA in the CNS. AAV vector delivery of the *ARSA* gene to the CNS ameliorates the disease phenotypes in a mouse model of the disease.[13,31,32] As a next step in clinical translation, the goal of this study was to evaluate the safety of an AAVrh.10 serotype vector coding for the human *ARSA* gene (AAVrh.10hARSA) using direct administration to the CNS white matter of NHPs. We tested the treatment vector at 2 doses (total low dose, 2.85×10^{10} gc, and high dose, 1.5×10^{12} gc), divided into 12 equal doses administered bilaterally to six sites in the cerebral white matter. The low dose was not associated with any adverse effects, validating the safety of delivery of AAVrh.10hARSA through intraparenchymal administration at this dose.

However, administration of a higher dose of AAVrh.10hARSA or AAVrh.10Null was associated with local pathologic findings at the site of AAV vector administration and some minor pathologic findings in the spinal cord. These observations set an upper limit to the dose that can be safely administered in concentrated deposits in the CNS parenchyma.

Therapeutic strategies for MLD

There are no approved therapies for MLD, but several approaches are being investigated, including enzyme replacement therapy (ERT), gene therapy by *ex vivo* transplantation of genetically modified hematopoietic stem cells (HSCs), and AAV-mediated gene therapy directly to the CNS.

For ERT, the blood–brain barrier likely necessitates administering the recombinant enzyme directly into the CSF.[33–35] Clinical trials of ARSA ERT have been carried out both by intravenous (NCT00418561, NCT00633139) or intrathecal (NCT01510028, NCT01887938) delivery. The intravenously delivered recombinant hARSA (Metazym, Shire Human Genetics Therapeutics) did not have an impact on clinical or biochemical markers of disease.[36] Evaluation of the safety and efficacy of intrathecal ERT with recombinant human ARSA (Shire, SHP611, now Takeda Pharmaceutical Company, TAK-611) was tested in 24 children with MLD in a dose ascending trial of intrathecally administered hARSA at 10, 30, and 100 mg dose, every other week for 38 weeks.[37,38] The data demonstrated that SHP611/TAK-611 was safe and well tolerated at all doses; however, biochemically only the 100 mg cohorts showed a meaningful reduction in CSF biomarkers bringing them within normal age-matched CSF ranges.[36,39]

While all cohorts continued to show neurological decline, the 100 mg dose cohorts had a slower rate of decline.[36] Ongoing clinical trials (TAK-611; NCT03771898) are assessing the safety and efficacy of intrathecal administration at an increased frequency of once a week and an increased dose of 150 mg. While intrathecal ERT for MLD

is showing some promise, the half-life of ARSA is 4 days which requires the hARSA to be given weekly or biweekly for the lifetime of the patient,[40] making compliance a challenge. In addition, 25% of the patients in the trial described above suffered a serious adverse event related to the implanted intrathecal delivery device.[36]

HSC transplantation of children with MLD stabilizes demyelination and delays disease progression in presymptomatic or early symptomatic stage patients with the juvenile form of MLD, but not those who are symptomatic.[41] The difficulty of finding matching donors and the potential for immunological complications limit its utility as a therapeutic modality.[42–44] A modification of this approach is the *ex vivo* correction of a patient's own HSCs (CD34+ cells isolated using plasmapheresis) with a lentiviral vector expressing human ARSA.[45,46] This strategy is based on the concept that the modified CD34+ cells will differentiate into the macrophage lineage which will migrate to the brain, where the genetically modified cells will differentiate into microglial cells that express and secrete ARSA which will be taken up by surrounding brain cells.[47–49]

Clinical trials (Phase I/II; NCT01560182 and NCT 03392987, Orchard Therapeutics in collaboration with Ospedale San Raffaele-Telethon Institute for Gene Therapy, Italy) tested infusions of autologous CD34+ cells transduced with lentiviral vector containing human ARSA cDNA administered intravenously at 4 to 18×10^6 cells/kg dose, with busulfan myeloablation conditioning of bone marrow.[45,46] Of the 9 MLD children treated in trials, 7/8 children treated when presymptomatic showed prevention of disease onset or halted disease progression compared with historical untreated control patients with early-onset disease, with progression similar to that of normally developing children in 6/8 subjects.[46] There was protection from CNS demyelination in 8/8 patients, with 3/8 showing amelioration of PNS abnormalities, with signs of remyelination at skin biopsy sites tested.[46] While promising, this strategy is limited to siblings of previously identified MLD patients to treat the disease at the presymptomatic or early symptomatic stage and the patient must undergo a myeloablative regimen before the treatment, which can be associated with toxicity.[42,50]

In vivo gene therapy using an AAV vector capitalizes on the biology of ARSA as a precursor protein that is secreted and taken up by neighboring cells, thus minimizing the challenge of delivering the vector DNA to all cells.[14,51–54] Direct CNS administration of AAVrh.10-hARSA to the CNS of a murine model of MLD has demonstrated biologic efficacy,[13] and biodistribution studies in NHPs have demonstrated effective widespread distribution in the CNS following administration to cerebral white matter using catheters depositing the vector at 12 sites.[14] In this NHP efficacy study, we demonstrated vector-derived ARSA (FLAG-tagged) enzymatic activity across the CNS at the 1.5×10^{12} gc total dose at 13 weeks

in NHP.[14] Together, these studies paved the path for assessing the safety of this therapeutic approach as the next step in clinical translation.

Safety of AAVrh.10hARSA administration to the CNS

In the present study, we examined the safety of AAVrh.10hARSA to deliver the human *ARSA* transgene to the CNS of normal NHPs. The low dose (total dose 2.85×10^{10} gc; 2.4×10^9 gc dose/site) of AAVrh.10hARSA was well tolerated. There were no long-term effects of the vector and/or surgery in this cohort. The only observed effect attributed to this treatment was a minimal-to-mild T cell and B cell infiltrate localized at the intracerebral injection sites that was reversible (not observed at week 52), findings that were corroborated by MRI. Other than these findings, administration of low dose AAVrh.10hARSA to the CNS of NHPs did not differ from the PBS-administered controls in any parameter of general assessment or comprehensive blood profile (CBC, chemistry panel). Blinded videotape analysis of NHP behavior presurgery and post-administration showed no discernible neurological differences between the AAVrh.10hARSA dosage groups and the PBS controls. Minor variable changes were not attributed to the AAVrh.10hARSA vector.

In contrast, the high dose (1.5×10^{12} gc total dose; 1.3×10^{11} gc/site) of AAVrh.10 delivered to the brain parenchyma white matter was associated with localized abnormalities at the sites of vector administration, with minor abnormalities in the spinal cord. These findings did not have clinical consequences on in-life data, CBC, serum chemistry, or behavior. The adverse effects observed in the CNS of animals treated with high dose of both the control AAVrh.10Null and AAVrh.10hARSA vectors suggest that the abnormalities resulted from the AAVrh.10 capsid, not the ARSA transgene. The higher levels of endotoxin in the AAVrh.10Null vector may have exacerbated the immune response in these local sites of vector infusion. The latest guidance from the FDA recommends a threshold of 0.2 EU/kg body weight/hour for acceptable levels of endotoxin for vectors to be used for CNS delivery.[55]

Both groups had moderate-to-large numbers of T cells, B cells, and microglial cells and/or activated macrophages infiltrating the brain at the sites of injection. This inflammatory response was localized to the catheter sites, not observed at regions 1 cm distal from the administration sites, suggesting a very local response. The spinal cord of 6 of the 12 animals in these two groups displayed minimal-to-mild white matter axonal degeneration. The abnormal findings were localized to the lateral funiculi in the spinal cords, which contain a mixture of sensory (ascending) and motor (descending) axons, projections of upper motor neurons located in the cerebral cortex or brain stem.[56–58] This finding is similar to the spinal cord findings reported by Hordeaux *et al.*[59] following intracisternal administration of

AAV9.hIDS (iduronate 2-sulfatase). These finding were not reversible (observed in all high dose NHPs at week 52). While no clinical sequelae were observed they could have the future potential to affect neurological function.

Consistent with the observations in the present study, Zerah *et al.*[60] carried out a NHP safety study of CNS administration of AAVrh.10hARSA to NHPs ($n = 14$) at two doses, low dose 2.2×10^{11} and high dose 1.1×10^{12} gc in divided doses (low dose 1.8×10^{10} gc/site; high dose 9.2×10^{10} gc/site), for 7 and 90 days.[60] This study concluded that there was no toxicity based on biological or clinical parameters at the low dose. ARSA activity exceeded the normal endogenous activity level by 14% to 31%. There were abnormalities localized to the sites of administration noted in the high dose cohort observed in the 3 month MRI T2 scans but no clinical sequelae, consistent with our observation at 2.4×10^9 gc/site.

This study concluded that direct intraparenchymal delivery of AAVrh.10hARSA of the 2.2×10^{11} gc dose (1.8×10^{10} gc/site) appears to be safe and effective for CNS delivery, supporting its clinical use in children affected with MLD.[60] In addition, as the high dose in each study, 1.1 and 1.5×10^{12} gc (9.2×10^{10}–1.25×10^{11} gc/site) resulted in pathology proximal to the sites of AAVrh.10hARSA administration; while the lower total doses, 2.2×10^{11} (1.8×10^{10} gc/site, Zerah *et al.*[60]) and 2.85×10^{10} gc (2.4×10^9 gc/site, current study), resulted in no toxicity, we recommend that direct intraparenchymal administration of AAVrh.10 in the clinic be limited to a range below the high dose used here with additional animal studies to evaluate the safety of a range for intermediate doses.

Translation to humans

Our collaborators Sevin *et al.*[54,61] carried out and concluded a small-scale phase 1/2, open-labeled, clinical trial (NCT01801709; ClinicalTrials.gov) to assess the safety and efficacy of AAVrh.10hARSA for treatment of early-onset forms of MLD. The route of administration used to deliver the AAVrh.10hARSA vector is the same intraparenchymal delivery to the cerebral white matter (at 12 sites, through six image-guided catheters with two deposits per track) as used in this study. This study administered AAVrh.10hARSA at two doses (1×10^{12} and 4×10^{12} gc, $n = 2$ subjects/dose; 8.3×10^{10} and 3.3×10^{11} gc/site) and evaluated the safety and efficacy of the gene therapy modality based on multiple clinical, neuropsychological, radiological, electrophysiological, and biological parameters.[61] There were measurable expression levels of ARSA activity in the CSF, but the treated children continued to deteriorate, similar to the natural history of the MLD disease.[61]

This lack of impact on disease progression[61] suggests that higher doses of AAVrh.10hARSA and/or different routes or combination of multiple routes of administration may be necessary in future clinical trials. In this context,

higher doses for direct intraparenchymal delivery are too high for localized brain parenchymal delivery; it is likely that higher doses of AAV administered to CNS will be necessary to achieve therapeutic impact for MLD. As alternative approaches, we and others have explored other routes of AAV vector delivery at higher doses using administration to the CSF leading to widespread AAV-mediated expression of transgenes.[17,62]

We have delivered AAVrh.10 expressing the *APOE2* transgene at doses of 5×10^{13} gc to the NHP CNS through intracisternal and intracerebroventricular routes, safely with biodistribution of the secreted *APOE2* across the CNS, leading to the initiation of a clinical trial for Alzheimer's disease (NCT03634007).[17] Taghian *et al.*[62] assessed intracisternal administration of AAVrh8-GFP at 1×10^{14} gc in sheep without any adverse effects and obtained widespread biodistribution across the CNS by 3 weeks.[62] Gray-Edwards *et al.*[63] using dual intracerebroventricular and intrathalamic routes in GM1-affected cats have shown that administration to the CSF plus CNS parenchyma could be efficacious, even at a relatively low dose of 5.4×10^{12} gc, whereas a single route of delivery to the CNS was not as effective. Based on these observations, it is possible that AAVrh.10 mediated gene therapy could be more effective if we could distribute the ARSA more widely in the CNS either by delivering the vector through the CSF alone or in combination with the intraparenchymal route.

AUTHORS' CONTRIBUTIONS

J.B.R.: conceived study, performed experimental work and data analysis/interpretation, prepared article. A.C., B.P.D.: performed experimental work and data analysis/interpretation, reviewed article for content. J.P.D., D.J.B.: performed data analysis/interpretation, reviewed article for content. S.M.: performed experimental work (Pathology necropsy) and data analysis/interpretation, participated in the study design, prepared article. R.J.R.A.: performed experimental work and reviewed article for content. R.G.C., D.S., S.M.K.: conceived study, performed data analysis/interpretation, prepared article.

SUPPLEMENTARY MATERIAL

Supplementary Data
Supplementary Figure S1
Supplementary Figure S2
Supplementary Figure S3
Supplementary Figure S4
Supplementary Figure S5
Supplementary Figure S6
Supplementary Figure S7
Supplementary Table S1
Supplementary Table S2

REFERENCES

1. von Figura K, Gieselmann V, Jaeken J. Metachromatic leukodystrophy. In: Scriver CR, Beaudet AL, Sly WS, Valle D, eds. The Metabolic and Molecular Bases of Inherited Disease. New York: McGraw-Hill, 2001:3695–3724.

2. Aubourg P, Sevin C, Cartier N. Mouse models of metachromatic leukodystrophy and adrenoleukodystrophy. In: De Deyn PP, Van Dam D, eds. Animal Models of Dementia, Neuromethods, vol. 48. Berlin, Germany: Springer Science+Business Media, LLC, 2011:493–513.

3. Batzios SP, Zafeiriou DI. Developing treatment options for metachromatic leukodystrophy. Mol Genet Metab 2012;105:56–63.

4. Rosenberg JB, Kaminsky SM, Aubourg P, et al. Gene therapy for metachromatic leukodystrophy. J Neurosci Res 2016;94:1169–1179.

5. Beerepoot S, Nierkens S, Boelens JJ, et al. Peripheral neuropathy in metachromatic leukodystrophy: current status and future perspective. Orphanet J Rare Dis 2019;14:240.

6. Gieselmann V, Krageloh-Mann I. Metachromatic leukodystrophy—an update. Neuropediatrics 2010;41:1–6.

7. Gieselmann V, Matzner U, Hess B, et al. Metachromatic leukodystrophy: molecular genetics and an animal model. J Inherit Metab Dis 1998;21:564–574.

8. Molander-Melin M, Pernber Z, Franken S, et al. Accumulation of sulfatide in neuronal and glial cells of arylsulfatase A deficient mice. J Neurocytol 2004;33:417–427.

9. Patil SA, Maegawa GH. Developing therapeutic approaches for metachromatic leukodystrophy. Drug Des Devel Ther 2013;7:729–745.

10. Sevin C, Aubourg P, Cartier N. Enzyme, cell and gene-based therapies for metachromatic leukodystrophy. J Inherit Metab Dis 2007;30:175–183.

11. Takahashi T, Suzuki T. Role of sulfatide in normal and pathological cells and tissues. J Lipid Res 2012;53:1437–1450.

12. Wittke D, Hartmann D, Gieselmann V, et al. Lysosomal sulfatide storage in the brain of arylsulfatase A-deficient mice: cellular alterations and topographic distribution. Acta Neuropathol 2004;108:261–271.

13. Piguet F, Sondhi D, Piraud M, et al. Correction of brain oligodendrocytes by AAVrh.10 intracerebral gene therapy in metachromatic leukodystrophy mice. Hum Gene Ther 2012;23:903–914.

14. Rosenberg JB, Sondhi D, Rubin DG, et al. Comparative efficacy and safety of multiple routes of

direct CNS administration of adeno-associated virus gene transfer vector serotype rh.10 expressing the human arylsulfatase A cDNA to nonhuman primates. Hum Gene Ther Clin Dev 2014;25: 164–177.

15. Chiuchiolo MJ, Kaminsky SM, Sondhi D, et al. Intrapleural administration of an AAVrh.10 vector coding for human alpha1-antitrypsin for the treatment of alpha1-antitrypsin deficiency. Hum Gene Ther Clin Dev 2013;24:161–173.

16. Hackett NR, Redmond DE, Sondhi D, et al. Safety of direct administration of AAV2(CU)hCLN2, a candidate treatment for the central nervous system manifestations of late infantile neuronal ceroid lipofuscinosis, to the brain of rats and nonhuman primates. Hum Gene Ther 2005;16: 1484–1503.

17. Rosenberg JB, Kaplitt MG, De BP, et al. AAVrh.10-mediated APOE2 central nervous system gene therapy for APOE4-associated Alzheimer's disease. Hum Gene Ther Clin Dev 2018;29:24–47.

18. Sondhi D, Johnson L, Purpura K, et al. Long-term expression and safety of administration of AAVrh.10hCLN2 to the brain of rats and nonhuman primates for the treatment of late infantile neuronal ceroid lipofuscinosis. Hum Gene Ther Methods 2012;23:324–335.

19. Souweidane MM, Fraser JF, Arkin LM, et al. Gene therapy for late infantile neuronal ceroid lipofuscinosis: neurosurgical considerations. J Neurosurg Pediatr 2010;6:115–122.

20. Drobeck HP, Mayes BA, Barbolt TA, et al. Subarachnoid administration of iohexol in cynomolgus monkeys. Acta Radiol Diagn (Stockh) 1986;27: 349–355.

21. Gilberto DB, Zeoli AH, Szczerba PJ, et al. An alternative method of chronic cerebrospinal fluid collection via the cisterna magna in conscious rhesus monkeys. Contemp Top Lab Anim Sci 2003; 42:53–59.

22. De BP, Heguy A, Hackett NR, et al. High levels of persistent expression of alpha1-antitrypsin mediated by the nonhuman primate serotype rh.10 adeno-associated virus despite preexisting immunity to common human adeno-associated viruses. Mol Ther 2006;13:67–76.

23. Lewis RW, Billington R, Debryune E, et al. Recognition of adverse and nonadverse effects in toxicity studies. Toxicol Pathol 2002;30:66–74.

24. Arnold DL, Bryce F, Karpinski K, et al. Toxicological consequences of Aroclor 1254 ingestion by female rhesus (Macaca mulatta) monkeys. Part 1B. Prebreeding phase: clinical and analytical laboratory findings. Food Chem Toxicol 1993;31: 811–824.

25. Liddie S, Goody RJ, Valles R, et al. Clinical chemistry and hematology values in a Caribbean population of African green monkeys. J Med Primatol 2010;39:389–398.

26. Woodward RA, Weld KP. A comparison of ketamine, ketamine-acepromazine, and tiletamine-zolazepam on various hematologic parameters in rhesus monkeys (Macaca mulatta). Contemp Top Lab Anim Sci 1997;36:55–57.

27. Markmann S, Christie-Reid JJ, Rosenberg JB, et al. Attenuation of the Niemann-Pick type C2 disease phenotype by intracisternal administration of an AAVrh.10 vector expressing Npc2. Exp Neurol 2018;306:22–33.

28. Qiu T, Chiuchiolo MJ, Whaley AS, et al. Gene therapy for C1 esterase inhibitor deficiency in a Murine Model of Hereditary angioedema. Allergy 2019;74:1081–1089.

29. Bailey SA, Zidell RH, Perry RW. Relationships between organ weight and body/brain weight in the rat: what is the best analytical endpoint? Toxicol Pathol 2004;32:448–466.

30. Nirogi R, Goyal VK, Jana S, et al. What suits best for organ weight analysis: review of relationship between organ weight and body/brain weight for rodent toxicity studies. IJPSR 2014;5:1525–1532.

31. Sevin C, Verot L, Benraiss A, et al. Partial cure of established disease in an animal model of metachromatic leukodystrophy after intracerebral adeno-associated virus-mediated gene transfer. Gene Ther 2007;4:405–414.

32. Sevin C, Benraiss A, Van Dam D, et al. Intracerebral adeno-associated virus-mediated gene transfer in rapidly progressive forms of metachromatic leukodystrophy. Hum Mol Genet 2006; 15:53–64.

33. Abbott NJ. Blood-brain barrier structure and function and the challenges for CNS drug delivery. J Inherit Metab Dis 2013;36:437–449.

34. Concolino D, Deodato F, Parini R. Enzyme replacement therapy: efficacy and limitations. Ital J Pediatr 2018;44:120.

35. Pardridge WM. CSF, blood-brain barrier, and brain drug delivery. Expert Opin Drug Deliv 2016;13: 963–975.

36. Dali C, Sevin C, Krageloh-Mann I, et al. Safety of intrathecal delivery of recombinant human arylsulfatase A in children with metachromatic leukodystrophy: results from a phase 1/2 clinical trial. Mol Genet Metab 2020;131:235–244.

37. Simonis H, Yaghootfam C, Sylvester M, et al. Evolutionary redesign of the lysosomal enzyme arylsulfatase A increases efficacy of enzyme replacement therapy for metachromatic leukodystrophy. Hum Mol Genet 2019;28:1810–1821.

38. Wright T, Li A, Lotterhand J, et al. Nonclinical comparability studies of recombinant human arylsulfatase A addressing manufacturing process changes. PLoS One 2018;13:e0195186.

39. Troy S, Wasilewski M, Beusmans J, et al. Pharmacokinetic modeling of intrathecally administered recombinant human arylsulfatase A (TAK-611) in children with metachromatic leukodystrophy. Clin Pharmacol Ther 2020;107:1394–1404.

40. Matzner U, Herbst E, Hedayati KK, et al. Enzyme replacement improves nervous system pathology and function in a mouse model for metachromatic leukodystrophy. Hum Mol Genet 2005;14:1139–1152.

41. Ohashi T. Gene therapy for lysosomal storage diseases and peroxisomal diseases. J Hum Genet 2019;64:139–143.

42. Gennery AR. The challenges presented by haematopoietic stem cell transplantation in children with primary immunodeficiency. Br Med Bull 2020; 135:4–15.

43. Lamsfus-Calle A, Daniel-Moreno A, Urena-Bailen G, et al. Hematopoietic stem cell gene therapy: the optimal use of lentivirus and gene editing approaches. Blood Rev 2020;40:100641.

44. Petrillo C, Calabria A, Piras F, et al. Assessing the impact of cyclosporin A on lentiviral transduction and preservation of human hematopoietic stem cells in clinically relevant ex vivo gene therapy settings. Hum Gene Ther 2019;30:1133–1146.

45. Biffi A, Montini E, Lorioli L, et al. Lentiviral hematopoietic stem cell gene therapy benefits metachromatic leukodystrophy. Science 2013;341: 1233158.

46. Sessa M, Lorioli L, Fumagalli F, et al. Lentiviral haemopoietic stem-cell gene therapy in early-onset metachromatic leukodystrophy: an ad-hoc analysis of a non-randomised, open-label, phase 1/2 trial. Lancet 2016;388:476–487.

47. Asheuer M, Pflumio F, Benhamida S, et al. Human CD34+ cells differentiate into microglia and express recombinant therapeutic protein. Proc Natl Acad Sci U S A 2004;101:3557–3562.

48. Biffi A, Capotondo A, Fasano S, et al. Gene therapy of metachromatic leukodystrophy reverses neurological damage and deficits in mice. J Clin Invest 2006;116:3070–3082.

49. Biffi A, De Palma M, Quattrini A, et al. Correction of metachromatic leukodystrophy in the mouse model by transplantation of genetically modified hematopoietic stem cells. J Clin Invest 2004;113: 1118–1129.

50. Morgan RA, Gray D, Lomova A, et al. Hematopoietic stem cell gene therapy: progress and lessons learned. Cell Stem Cell 2017;21:574–590.

51. Funk B, Kessler U, Eisenmenger W, et al. Expression of the insulin-like growth factor-II/mannose-6-phosphate receptor in multiple human tissues during fetal life and early infancy. J Clin Endocrinol Metab 1992;75:424–431.

52. Ghosh P, Dahms NM, Kornfeld S. Mannose 6-phosphate receptors: new twists in the tale. Nat Rev Mol Cell Biol 2003;4:202–212.

53. Willingham MC, Pastan IH, Sahagian GG, et al. Morphologic study of the internalization of a lysosomal enzyme by the mannose 6-phosphate receptor in cultured Chinese hamster ovary cells. Proc Natl Acad Sci U S A 1981;78:6967–6971.

54. Aubourg P. Gene therapy for leukodystrophy: progress, challenges and opportunities. Exp Opin Orph Drugs 2016;4:359–367.

55. Food and Drug Administration. Setting Endotoxin Limits During Development of Investigational On-

cology Drugs and Biological Products: Guidance for Industry (DRAFT GUIDANCE). 2020. Available at: https://www.fda.gov/regulatory-information/search-fda-guidance-documents/setting-endotoxin-limits-during-development-investigational-oncology-drugs-and-biological-products (last accessed February 24, 2021).

56. Cregg JM, Leiras R, Montalant A, et al. Brainstem neurons that command mammalian locomotor asymmetries. Nat Neurosci 2020;23:730–740.

57. Morecraft RJ, Ge J, Stilwell-Morecraft KS, et al. New corticopontine connections in the primate brain: contralateral projections from the arm/hand area of the precentral motor region. Front Neuroanat 2018;12:68.

58. Wang Z, Maunze B, Wang Y, et al. Global connectivity and function of descending spinal input revealed by 3D microscopy and retrograde transduction. J Neurosci 2018;38:10566–10581.

59. Hordeaux J, Hinderer C, Goode T, et al. Toxicology study of intra-cisterna magna adeno-associated virus 9 expressing iduronate-2-sulfatase in rhesus macaques. Mol Ther Methods Clin Dev 2018;10: 68–78.

60. Zerah M, Piguet F, Colle MA, et al. Intracerebral gene therapy using AAVrh.10-hARSA recombinant vector to treat patients with early-onset forms of metachromatic leukodystrophy: preclinical feasibility and safety assessments in nonhuman primates. Hum Gene Ther Clin Dev 2015;26:113–124.

61. Sevin C, Roujeau T, Cartier N, et al. Intracerebral gene therapy in children with metachromatic leukodystrophy: results of a phase I/II trial. Mol Genet Metab 2018;123:S129.

62. Taghian T, Marosfoi MG, Puri AS, et al. A safe and reliable technique for CNS delivery of AAV vectors in the cisterna magna. Mol Ther 2020;28:411–421.

63. Gray-Edwards HL, Maguire AS, Salibi N, et al. 7T MRI predicts amelioration of neurodegeneration in the brain after AAV gene therapy. Mol Ther Methods Clin Dev 2020;17:258–270.